

Interference of extratropical surface climate anomalies induced by El Niño and stratospheric sudden warmings

Masakazu Taguchi¹ and Dennis L. Hartmann

Department of Atmospheric Sciences, University of Washington, Seattle, Washington, USA

Received 15 November 2004; revised 9 January 2005; accepted 25 January 2005; published 23 February 2005.

[1] The El Niño/Southern Oscillation (ENSO) and stratospheric sudden warmings (SSWs) each induce significant surface climate anomalies in Northern latitudes during winter. Nonetheless, possible connections between the impacts of the ENSO and SSWs remain relatively unexplored. Using both observational analysis and global climate model (GCM) experiments, we show that the impacts of El Niño and SSWs interfere over North America. The interference includes constructive interference, or synergistic impacts of the El Niño and SSWs over the southeastern US through northern Mexico, resulting in enhancement of colder and wetter climate when El Niño and SSWs occur in the same winter. The interference is of practical importance such as in extended-range weather forecasts, since the impacts of the two phenomena affect seasonal averages and increase the probability of extreme weather conditions in the region. **Citation:** Taguchi, M., and D. L. Hartmann (2005), Interference of extratropical surface climate anomalies induced by El Niño and stratospheric sudden warmings, *Geophys. Res. Lett.*, 32, L04709, doi:10.1029/2004GL022004.

1. Introduction

[2] Extratropical tropospheric and surface climate variability on seasonal and interannual timescales arises from external forcings as well as from internal processes. It is well known that inherent variability of the atmosphere-ocean coupled system in the tropical Pacific region (ENSO) is the largest source of interannual climate variability around the globe [e.g., Glantz, 2001; Wallace, 1994]. The downstream response to anomalous sea surface temperatures (SSTs), rainfall and atmospheric heating in the tropical Pacific during El Niño conditions includes wetter and colder climate of the SE US and northern Mexico during Northern Hemisphere (NH) winter [e.g., Horel and Wallace, 1981; Hoskins and Karoly, 1981; Ropelewski, 1992].

[3] Recent studies have suggested that the surface climate is also influenced by occurrence of SSWs [Baldwin *et al.*, 2003a; Hartmann *et al.*, 2000]. Circulation anomalies following SSWs tend to propagate downward from the stratosphere to the surface, where the climate exhibits sea-level pressure anomalies that resemble the negative phase of the Northern Annular mode (NAM) [Baldwin and Dunkerton, 1999, 2001; Limpasuvan *et al.*, 2004]. The NAM, also called

the Arctic Oscillation and closely related to the North Atlantic Oscillation, is a dominant mode of low-frequency variability of the extratropical troposphere, characterized by synchronous fluctuations in pressure with opposite signs between mid- and high latitudes [Thompson and Wallace, 1998, 2000]. Numerical experiments are used to show that SSWs can actually induce surface climate anomalies [e.g., Taguchi, 2003].

[4] No study has investigated possible connections between the surface climate impacts of ENSO and SSWs, although both affect planetary-scale flow in NH winter extratropics. Some studied ENSO's impact on the NAM and the stratospheric circulation [Quadrelli and Wallace, 2002; Labitzke and van Loon, 1999; Hamilton, 1995; Sassi *et al.*, 2004]. The two forcings are also considered separately in applications to weather prediction [Wallace, 1994; Baldwin *et al.*, 2003b]. Here we explore possible interference of climate anomalies induced by the ENSO and SSWs through both observational analysis and idealized GCM experiments.

2. Observational Analysis

[5] Our observational analysis makes use of daily NCEP/NCAR (National Centers for Environmental Prediction and the National Center for Atmospheric Research) reanalysis data of 55 NH winters (December to February) from 1948/1949 to 2002/2003 [Kalnay *et al.*, 1996]. We also used "cold-tongue index (CTI)" of anomalous SSTs in the tropical Pacific (180°W–90°W and 6°N–6°S) averaged over the NH winter season. The CTI data is provided by Joint Institute for the Study of the Atmosphere and the Oceans at the University of Washington.

[6] Our analysis aims to separate the effects of ENSO and SSW events on North American winter climate by dividing the sample into four regimes defined by whether ENSO is warm or cold and whether an SSW has occurred or not (Table 1). For the ENSO state, we classified "El Niño" and "La Niña" winters as those of the 10 highest and lowest values of the CTI, respectively. To determine when an SSW has occurred, we used temperature time series at the North Pole and 10 hPa. We searched for periods when the temperature becomes 30 K warmer than its mean seasonal march and defined key date of each SSW period as the day on which the anomalous temperature achieved its maximum value. We obtained 35 SSWs in the 55 winters, with 6 and 9 in the 10 La Niña and 10 El Niño winters, respectively. We then defined a "post-SSW period" as the period from 11 to 60 days after the key date of each SSW. It is in this period that SSWs have their strongest impact on the surface climate according to existing studies [Baldwin and Dunkerton, 2001;

¹Now at Research Institute for Sustainable Humanosphere, Kyoto University, Gokasyo, Uji, Japan.

Table 1. Four Regimes I to IV Defined in Terms of ENSO and Stratospheric Conditions

	La Niña	El Niño
Quiet Stratosphere	I	II
Post-SSW	III	IV

[Limpasuvan *et al.*, 2004] and our preliminary composite of all 35 SSWs. We also defined a “quiet-stratosphere period” as days that do not fall in a period between 40 days before and 70 days after any SSW. The regimes I and II (III and IV) include days in the quiet-stratosphere period (post-SSW period) of the La Niña and El Niño winters, respectively (Table 1).

[7] The difference, regime II minus regime I, measures the response to the El Niño forcing when the stratosphere is quiescent (Figure 1a). It is the best estimate for ENSO’s impact that arises within the troposphere. The response is consistent with previous analyses of ENSO’s impact in mid-latitudes [e.g., Ropelewski, 1992] in that it shows colder and wetter climate over the SE US to northern Mexico, accompanied by decline of geopotential height Z300 at an upper tropospheric level 300 hPa above the central and southern US. The climate anomalies change in some regions when the El Niño and SSWs occur together (Figure 1b, difference IV minus I) compared to the El Niño conditions without SSWs (Figure 1a). The change is, in principle, equal to the impact of the SSWs during the El Niño winters (Figure 1c, difference IV minus II). The response to the SSWs alone is similar to the negative phase of the NAM as observed [Limpasuvan *et al.*, 2004]. It is also clear that the impact of the SSWs is generally comparable in magnitude in the US to that of the El Niño. The climate anomalies in each panel indicate that strong cooling of near-surface temperature T_s occurs below a strong decline of Z300 while precipitation R is enhanced equatorward of the anomalously low Z300.

[8] The results in Figures 1a–1c are only statistically significant at a limited confidence level, because the observational record is not long enough and because it also includes effects of other factors, such as the quasi-biennial oscillation, global warming, and so on. The results nonetheless suggest constructive interference between the impacts of the ENSO and SSWs around the US Gulf coast, where both forcings act in the same sense (diagonal lines toward bottom-left show constructive interference in Z300 between Figures 1a and 1c with a 75% level). On the other hand, the El Niño and SSWs may interfere destructively, for example, around the northeastern US. We can gain confidence in our observations by showing that a GCM produces responses to ENSO and SSWs with a higher level that are very similar to those observed.

3. GCM Experiments

[9] Our numerical experiments employ the Whole Atmosphere Community Climate model (WACCM), a version of NCAR Community Climate Model that is extended to include the middle and upper atmosphere [Sassi *et al.*, 2002]. The horizontal resolution is T63, with 66 vertical levels from the surface up to about 110 km. The experiments consist of two runs forced with perpetual January conditions, including prescribed climatological SST and

ozone distributions. In one case the SSTs in the eastern tropical Pacific are raised (called WARM), and they are lowered in the other (called COLD) to introduce an ENSO-like SST forcing with a peak difference about 2.5°C . Perpetual January runs are an economical tool to compute climate anomalies characteristic of NH winter. SSWs are internally generated in both runs. The two runs each include

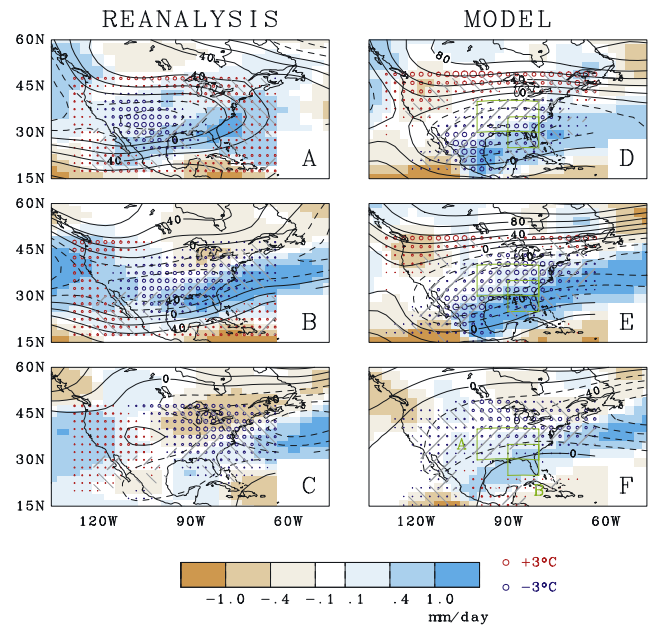


Figure 1. Composite differences for three combinations of the regimes in the observations and GCM experiments. The panels a to c are for the observations; (a) II minus I, impact of ENSO in the quiet-stratosphere period, (b) IV minus I, impacts of ENSO and stratospheric forcings, and (c) IV minus II, impact of the SSWs in the El Niño winters. The panels d, e and f are model counterparts of a, b, and c, respectively. Contours are for geopotential height at 300 hPa, Z300, with a contour interval of 20 m. Red and blue circles are for near-surface temperature, T_s , with red (blue) indicating warming (cooling). Size of the circles is proportional to their magnitude, with examples of $\pm 3^\circ\text{C}$ given below the panels. Only values over ± 0.2 in a region of 60°W – 130°W and 15°N – 50°N are plotted. Blue and orange shadings are for precipitation rate, R (mm day^{-1}), with color codes also given below. Gray diagonal lines show that the Z300 impact of the SSWs in the El Niño condition is statistically significant at a confidence level of 75% for the observations (panel c) and 95% for the GCM results (panel f). For the statistical test of the observed (modeled) SSWs’ impact, Student’s t test is applied to 9 (41) values of Z300 in the post-SSW period after the 9 (41) SSWs in the El Niño winters (run WARM) at each gridpoint. Statistical significance of the ENSO’s impact (panels a and d) is much higher, as the ENSO forcing persists longer. Diagonal lines toward the bottom-left (bottom-right) show that the Z300 impact of the SSWs is in the same (opposite) sense as that of the ENSO. Green boxes A and B in the panel f denote regions for the spatial averages used in Figure 2; box A covers a region of 80°W – 100°W and 30°N – 40°N , while box B is for 80°W – 90°W and 25°N – 35°N .

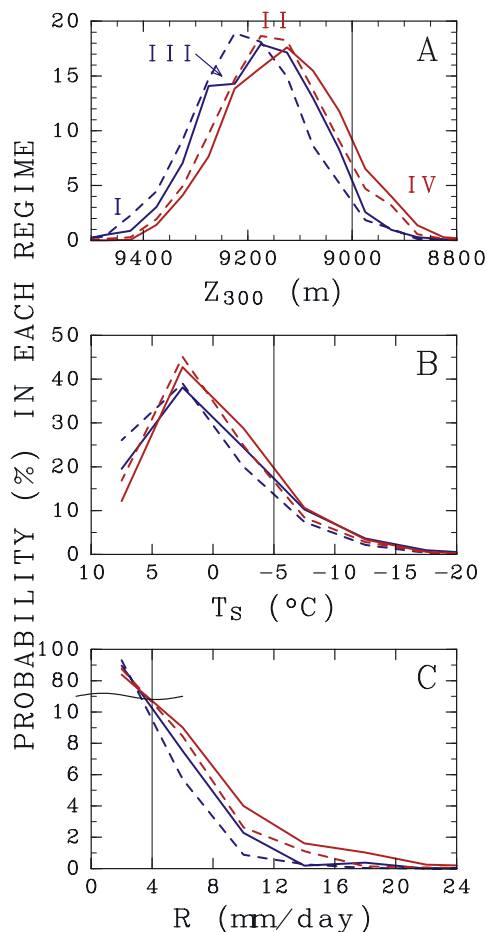


Figure 2. PDFs in the regimes I through IV in the GCM experiments; (a) Z300, (b) Ts, and (c) R, where Z300 and Ts are averaged in the box A and R in the box B shown in Figure 1. Broken and solid lines in blue (red) are for regimes I and III (II and IV), respectively, as shown in the panel a. Black vertical lines denote three thresholds of extreme weather conditions used in Table 2.

240 months of equilibrated January climate. The experiments thus afford a larger sample than is available from observations, and yield more statistically reliable results.

[10] We applied a similar four-regime composite analysis to the model data (Table 1). We populated the four regimes using the WARM and COLD experiments for El Niño and La Niña, and the same definitions for the quiet-stratosphere and post-SSW periods. We identified 21 and 41 SSWs in the runs COLD and WARM, respectively, using the time series of the zonal mean temperature [T] at 88°N and 11 hPa. The criteria for the model SSWs are a 205 K baseline and 235 K threshold for SSW key dates. The modeled responses (Figures 1d–1f) are very consistent with the observations (Figures 1a–1c) and show constructive interference over the SE US and northern Mexico much more clearly. Both El Niño and SSWs produce a colder and wetter climate associated with Z300 decline (Figures 1d–1f), and their superposition produces a much amplified response (Figure 1e). The statistical significance of the modeled constructive interference is obtained at a 95% level. The changes of the surface anomalies between regimes II and IV are an effect of the SSWs since only the previous occur-

rence of an SSW distinguishes the two regimes. The causality is also supported by a global version of Figure 1 (not displayed); only the difference between regimes II and I shows the PNA wave train while that between regimes IV and II resembles the observed tropospheric response to SSWs [Limpasuvan *et al.*, 2004].

[11] We further examined the modeled constructive interference in terms of probability distribution functions (PDFs) by using three indices that represent weather conditions in the SE US. The box A is used to take spatial averages of Z300 and Ts, while R is averaged in the box B as shown in Figure 1f. These boxes are chosen because the response to each forcing is large there, but the results are not sensitive to their slight changes. Consistently with the changes in the composite means, the PDFs systematically have more samples for lower height, surface cooling, and more precipitation, as the ENSO and stratospheric forcings are applied in turn (Figure 2); from regime I to II when the SST forcing is applied and from regime II to IV when the SSWs also occur.

[12] It is important to note that the PDFs have increased probability of extreme conditions as the two impact are added, although their shapes seem roughly similar. For example, the cumulated probability for $T_s \leq -5^\circ\text{C}$ is 9.9% for regime I, and it increases to 11.7% in regime II and further to 14.6% in regime IV. The other indices show similar tendencies toward increased probability of extreme weather when the ENSO and SSWs occur together (Table 2). A Monte Carlo simulation shows that the change in the cumulated probability is highly statistically significant. In the simulation, we randomly chose samples from all data in the two runs for three groups that had the same sizes as the regimes I, II and IV, and calculated the cumulated probability for the three thresholds. The difference in the cumulated probability between the regimes (Table 2) happened by chance in only 19 of the total 10,000 trials for Ts and in none for Z300 and R.

4. Discussion

[13] In summary, we have presented both observational and modeling results to show significant interference of extratropical surface climate anomalies induced by El Niño and SSWs. The impacts of the El Niño and SSWs each are robust and can basically add to each other. The consistency between the observational and modeling results provides a convincing case that El Niño and SSWs exert synergistic impacts to enhance colder and wetter winter climate over the SE US and northern Mexico. It will be of interest to ask whether or not models without a well-resolved stratosphere

Table 2. Cumulated Probability (%) in the Regimes I to IV of the GCM Experiments for Three Thresholds of Extreme Weather Conditions (Left to Right) $Z300 \leq 9000$ m, $T_s \leq -5^\circ\text{C}$, and $R \geq 4$ mm day⁻¹a

	$Z300 \leq 9000$ m	$T_s \leq -5^\circ\text{C}$	$R \geq 4$ mm day ⁻¹
I	3.1	9.9	6.9
II	8.6	11.7	12.4
III	3.9	15.0	10.4
IV	12.3	14.6	16.0

^aHere, Z300 and Ts are averaged in the box A, while R is in the box B shown in Figure 1f.

can simulate such extreme weather conditions in the SE US as produced by WACCM. This work suggests the potential to increase understanding and forecasting of surface climate variability by taking account of both ENSO and SSWs. For example, this interference is of great interest in extended-range weather forecasts, since the impacts of the El Niño and SSWs affect seasonal means and their synergism can increase the frequency of extreme weather conditions. It also seems clear that physical models used to project the response of extratropical climate to tropical SSTs must have a realistic stratosphere and be able to forecast SSWs in order to obtain the correct distribution of the climate anomalies.

[14] **Acknowledgments.** We thank the developers at NCAR for the use of WACCM. We also thank Marc L. Michelsen for assisting our model runs. The present graphic tools were based on the codes in the GFD-DENNOU Library. This work is supported by the NSF under Climate Dynamics Grants ATM-0332269 and ATM-9873691 to the University of Washington.

References

- Baldwin, M. P., and T. J. Dunkerton (1999), Propagation of the Arctic oscillation from the stratosphere to the troposphere, *J. Geophys. Res.*, *104*, 30,937–30,946.
- Baldwin, M. P., and T. J. Dunkerton (2001), Stratospheric harbingers of anomalous weather regimes, *Science*, *294*, 581–584.
- Baldwin, M. P., D. W. J. Thompson, E. F. Shuckburgh, W. A. Norton, and N. P. Gillett (2003a), Weather from the stratosphere?, *Science*, *301*, 317–318.
- Baldwin, M. P., et al. (2003b), Stratospheric memory and extended-range weather forecasts, *Science*, *301*, 636–640.
- Glantz, M. H. (2001), *Currents of Change*, 252 pp., Cambridge Univ. Press, New York.
- Hamilton, K. (1995), Interannual variability in the Northern Hemisphere winter middle atmosphere in control and perturbed experiments with the GFDL SKYHI general circulation model, *J. Atmos. Sci.*, *52*, 44–66.
- Hartmann, D. L., J. M. Wallace, V. Limpasuvan, D. W. J. Thompson, and J. R. Holton (2000), Can ozone depletion and global warming interact to produce rapid climate change?, *Proc. Natl. Acad. Sci. U. S. A.*, *97*, 1412–1417.
- Horel, J. D., and J. M. Wallace (1981), Planetary-scale atmospheric phenomena associated with the Southern Oscillation, *Mon. Weather Rev.*, *103*, 813–829.
- Hoskins, B. J., and D. J. Karoly (1981), The steady linear response of a spherical atmosphere to thermal and orographic forcing, *J. Atmos. Sci.*, *38*, 1179–1196.
- Kalnay, E., et al. (1996), The NCEP/NCAR 40-year reanalysis project, *Bull. Am. Meteorol. Soc.*, *77*, 437–472.
- Labitzke, K., and H. van Loon (1999), *The Stratosphere*, 179 pp., Springer, New York.
- Limpasuvan, V., D. W. J. Thompson, and D. L. Hartmann (2004), The life cycle of the Northern Hemisphere sudden stratospheric warmings, *J. Clim.*, *17*, 2584–2596.
- Quadrelli, R., and J. M. Wallace (2002), Dependence of the structure of the Northern Hemisphere annular mode on the polarity of ENSO, *Geophys. Res. Lett.*, *29*(23), 2132, doi:10.1029/2002GL015807.
- Ropelewski, C. F. (1992), Predicting El Niño events, *Nature*, *356*, 476–477.
- Sassi, F., R. R. Garcia, B. A. Boville, and H. Liu (2002), On temperature inversions and the mesospheric surf zone, *J. Geophys. Res.*, *107*(D19), 4380, doi:10.1029/2001JD001525.
- Sassi, F., D. Kinnison, B. A. Boville, R. R. Garcia, and R. Roble (2004), Effect of El Niño–Southern Oscillation on the dynamical, thermal, and chemical structure of the middle atmosphere, *J. Geophys. Res.*, *109*, D17108, doi:10.1029/2003JD004434.
- Taguchi, M. (2003), Tropospheric response to stratospheric sudden warmings in a simple global circulation model, *J. Clim.*, *16*, 3039–3049.
- Thompson, D. W. J., and J. M. Wallace (1998), The Arctic oscillation signature in the wintertime geopotential and temperature fields, *Geophys. Res. Lett.*, *25*, 1297–1300.
- Thompson, D. W. J., and J. M. Wallace (2000), Annular modes in the extratropical circulation. Part I: Month-to-month variability, *J. Clim.*, *13*, 1000–1016.
- Wallace, J. M. (1994), *Reports to the Nation on Our Changing Planet*, Univ. Corp. for Atmos. Res., Boulder, Colo.

D. L. Hartmann, Department of Atmospheric Sciences, University of Washington, Seattle, WA 98185-1640, USA.

M. Taguchi, Research Institute for Sustainable Humanosphere, Kyoto University, Gokasyo, Uji, 611-0011, Japan. (taguchi@atmos.washington.edu)